

Molecular dynamics simulation with reversible heat addition

Nicolas G. Hadjiconstantinou*

Department of Mechanical Engineering, Massachusetts Institute of Technology, Cambridge, Massachusetts 02139

(Received 22 September 1998)

We present a method developed to simulate heat addition in molecular dynamics simulations. The heat addition is shown to be *thermodynamically reversible*. Molecular dynamics simulations verify the applicability of the method and the reversibility of the heat addition. Constant pressure simulations indicate that the method is able to capture the dynamics of phase change. [S1063-651X(99)50301-2]

PACS number(s): 02.70.Ns, 64.60.-i, 05.70.Fh, 31.15.Qg

In this work we use the Gaussian principle of least constraint [1,2] to derive equations of motion that simulate heat addition (modeling, for example, internal heat generation due to the passage of electrical current through an electrolyte). The equations of motion for the heat addition are obtained by incorporating the constraint

$$\frac{1}{2} \sum_i \left(\frac{\vec{p}_i^2}{m_i} + \sum_{j \neq i} V(\vec{q}_{ij}) \right) = E_0 + N \int_0^t \dot{Q}(t) dt \quad (1)$$

in the Newtonian equations of motion in the Gaussian least constraint sense [2]. Here E_0 is the initial energy of all the particles, N is the number of particles, and $\dot{Q}(t)$ is the rate at which energy is added per particle. (In systems with mean flow an appropriate thermal energy must be considered.) The resulting equation of motion is

$$\dot{\vec{p}}_i = -\nabla \sum_{j \neq i} V(\vec{q}_{ij}) - \lambda(p) \vec{p}_i, \quad (2)$$

where

$$\lambda(p) = -\frac{N\dot{Q}(t)}{\sum_i \vec{p}_i^2/m_i}. \quad (3)$$

Although the above equations have been formulated to allow a heat addition rate that varies as a function of time [$\dot{Q}(t)$], in our simulations we will be using a constant heat addition \dot{Q} .

It can easily be shown that in the case of small heat addition the above equations can be linearized to the following algorithm:

$$\dot{\vec{p}}_i' = -\nabla \sum_{j \neq i} V(\vec{q}_{ij}) \quad (4)$$

and

$$\vec{p}_i = -[\lambda(p')\Delta t - 1] \vec{p}_i', \quad (5)$$

which is similar to the rescaling algorithm widely used to remove heat (although in a constant temperature formula-

tion) from simulations [3]. Here Δt is the numerical integration timestep.

It has been shown [2] that the constant temperature constraint equations resulting from the application of the Gaussian principle of least constraint indeed reproduce the correct (canonical ensemble) dynamics in the equilibrium case. Care, however, has to be taken in nonequilibrium situations since there has been no extension of the above result in the latter case. We expect that, since both sets of equations, (2) and (3) or (4) and (5), reduce to the Newtonian equations of motion for $\lambda \rightarrow 0$, the model dynamics will not be significantly different than the “correct” nonequilibrium dynamics for small λ . We remark that our model interprets heat addition as an acceleration in the direction of the velocity \vec{p}_i/m_i of the molecule. Despite the perhaps nonphysical nature of this interpretation, we believe that if the heat addition rate is small enough, or equivalently, the heat addition timescale is long enough compared to the collision time scale (τ), then complete thermalization of the added energy will occur sufficiently fast for the system to be in the “correct” nonequilibrium state at every instant in time. An estimate for the heat addition timescale (based on the heating rates used in this work) is $\tau_Q \sim 100\tau \gg \tau$; we thus conclude that the assumption of complete thermalization is valid.

Under the above assumption we can show that the mechanism proposed above is reversible in the thermodynamic sense. (It is obviously time reversible in the mechanical sense.) Using the general (compressible and incompressible) form of the Liouville theorem

$$\frac{\partial f}{\partial t} = -\sum_i^{3N} \left[\frac{\partial[\dot{q}_i f(q,p)]}{\partial q_i} + \frac{\partial[\dot{p}_i f(q,p)]}{\partial p_i} \right], \quad (6)$$

we obtain the following equation for the “Lagrangian” time dependence of the distribution function [4]

$$\frac{df}{dt} = -f \sum_i^{3N} \left[\left(\frac{\partial \dot{q}_i}{\partial q_i} \right) + \left(\frac{\partial \dot{p}_i}{\partial p_i} \right) \right], \quad (7)$$

or equivalently,

$$\frac{d \ln f}{dt} = -\sum_i^{3N} \left[\left(\frac{\partial \dot{q}_i}{\partial q_i} \right) + \left(\frac{\partial \dot{p}_i}{\partial p_i} \right) \right]. \quad (8)$$

*Electronic address: ngh@mit.edu

Substituting Eqs. (2) and (3) into Eq. (8) and neglecting

$$\frac{\partial \left(\sum_j \frac{\vec{p}_j^2}{m_j} \right)^{-1}}{\partial p_i} \sim \frac{1}{N},$$

we obtain

$$\frac{d \ln f}{dt} = - \sum_i^{3N} \frac{N \dot{Q}(t)}{3NkT} = - \frac{N \dot{Q}(t)}{kT}, \quad (9)$$

where k is Boltzmann's constant. This, in turn, yields

$$\frac{dS}{dt} = -k \frac{d \langle \ln f \rangle}{dt} = \frac{N \dot{Q}(t)}{T}, \quad (10)$$

which corresponds to reversible heat addition in the *thermodynamic sense*.

Note that the fundamental relation

$$dE = TdS - PdV \quad (11)$$

guarantees that for constant volume energy addition all final energy states can be reached by reversible heat addition, or in other words,

$$S(E+Q, V) = S(E, V) + \int_Q \frac{dQ}{T}. \quad (12)$$

We performed molecular dynamics (MD) simulations to verify that the equations of motion derived above indeed can be used to add heat in a reversible manner. The interaction potential used in all our simulations is the well known Lennard-Jones potential [5]

$$V(q) = 4\epsilon [(\sigma/q)^{12} - (\sigma/q)^6],$$

where q is the separation of the two interacting molecules. The potential is truncated at a distance (cut-off length) $q_c = 3\sigma$. Unless otherwise stated, all quantities will be expressed in reduced units using $\sigma = 3.4 \text{ \AA}$ for length, $m = 40 \text{ amu}$ for mass, $\epsilon/k = 119.8 \text{ }^\circ\text{K}$ for temperature, and $\tau = (m\sigma^2/48\epsilon)^{1/2} = 3.112 \times 10^{-13} \text{ s}$ for time. Here σ and ϵ are the parameters of the Lennard-Jones (LJ) potential for argon [5], m is the mass of the argon atom, and τ is the characteristic time for argon. The equations of motion (2) and (3) [or the rescaling equivalent (4) and (5)] are numerically integrated using Beeman's modified equations of motion [6], which is a fourth order accurate in space and third order accurate in time predictor corrector method. The evaluation of macroscopic properties (energy E , temperature T , pressure P , and density ρ) follows from the usual [7] definitions for statistical mechanical systems. Additionally, all extensive properties (energy E , heat addition rate \dot{Q} , entropy S , and Gibbs free energy G) will be given in specific (per unit mass) reduced units. Thermodynamic properties as functions of time are defined as "quasistatic" averages over intervals of 16τ .

A cluster of 3840 argon molecules is thermally equilibrated ($\dot{Q}=0$) at temperature $T=1$ and $\rho=0.7\sigma^{-3}$ ($P=0.07\epsilon/\sigma^3$) for a period of 320τ . Following the equilibra-

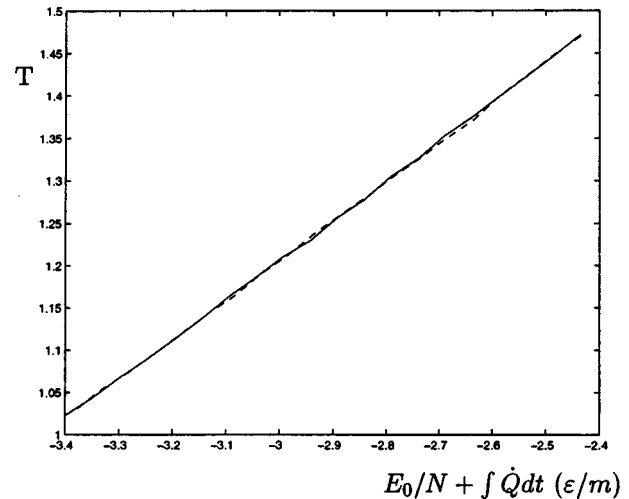


FIG. 1. Temperature as a function of heat added (solid line). The dashed line shows the reverse process.

tion period the fluid is heated with $\dot{Q} = 3.125 \times 10^{-3} \epsilon/(m\tau)$ for a further 320τ . Figure 1 shows the temperature history as a function of the heat added. On the same graph we show the path of the fluid during 320τ of simulation with $\dot{Q} = -3.125 \times 10^{-3} \epsilon/(m\tau)$. We see that the path is indeed reversible, as expected.

Constant pressure simulations are preferable because they facilitate the direct "thermodynamic connection" to the constant pressure phase change of fluids which both simplifies analysis, but is also more frequently observed. We now describe constant pressure simulations with heat addition. The pressure was kept constant by using the method of Parinello and Rahman [8]. Although the incorporation of the heat addition term $[\lambda(p)\vec{p}_i]$ in the general constant pressure framework of Parinello and Rahman [8] is the subject of future work, as is the proof of the thermodynamic reversibility of the resulting mechanism, in our simulations the two processes (heat addition and constant pressure volume change) were decoupled and hence applied sequentially. Our results indicate that the above assumption is acceptable, since excellent agreement is found with both experimental data and other simulations. Application of the linearized (rescaling) algorithm of equations (4) and (5) gives identical results (see later) that indicates that $\lambda(p)$ is indeed small, and possibly explains the decoupling of the heat addition and constant pressure processes.

A cluster of 480 argon atoms is thermally equilibrated at constant pressure ($P=0.07\epsilon/\sigma^3$) and zero heat addition ($\lambda=0$) for a period of 320τ . The simulation box is initially cubic with side $\Lambda = 8.95\sigma$ ($\rho=0.7\sigma^{-3}$) and fully periodic. After the equilibration period, the exact equations of heat addition (2) and (3) are integrated to simulate heating of the fluid at the same constant pressure with $\dot{Q} = 3.125 \times 10^{-3} \epsilon/(m\tau)$.

Figure 2 shows the temperature and density of the fluid as a function of time after heating starts. The liquid spinodal point is denoted C, and the vapor spinodal point is denoted F. We have made sure that the temperature is reasonably uniform within and between the two phases, to ensure that the above observed behavior is not due to some thermal instability associated with the heating mechanism.

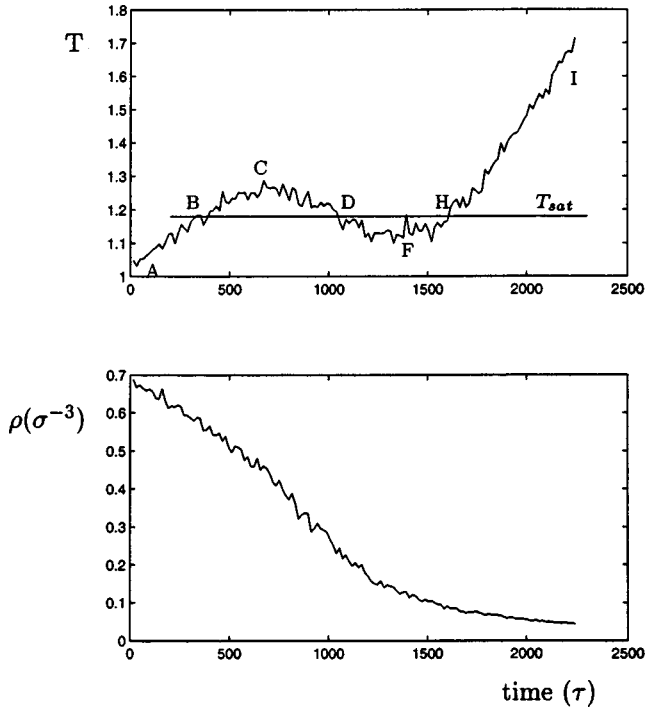


FIG. 2. Temperature and density of the fluid as a function of time after heating starts.

Figure 3 shows the numerical integration results for the entropy S and the Gibbs free energy $G = E - TS + PV$ as a function of temperature. The entropy S is evaluated by numerically integrating

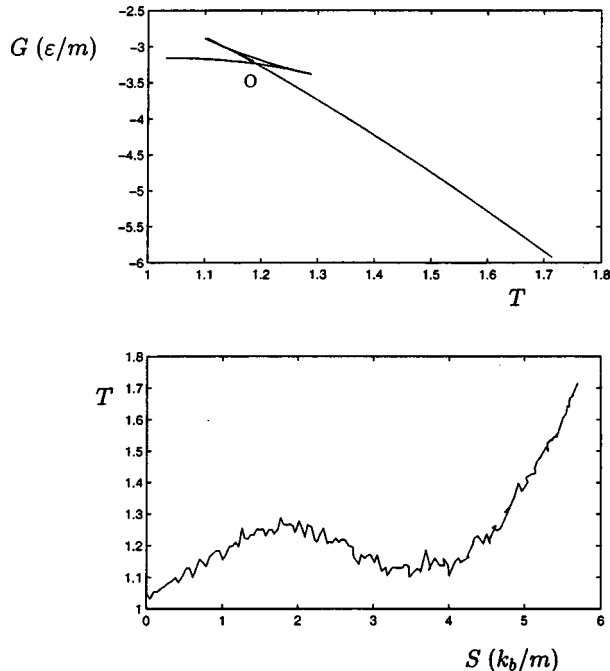


FIG. 3. Gibbs free energy as a function temperature (top) and temperature as a function of entropy (bottom) during the phase change.

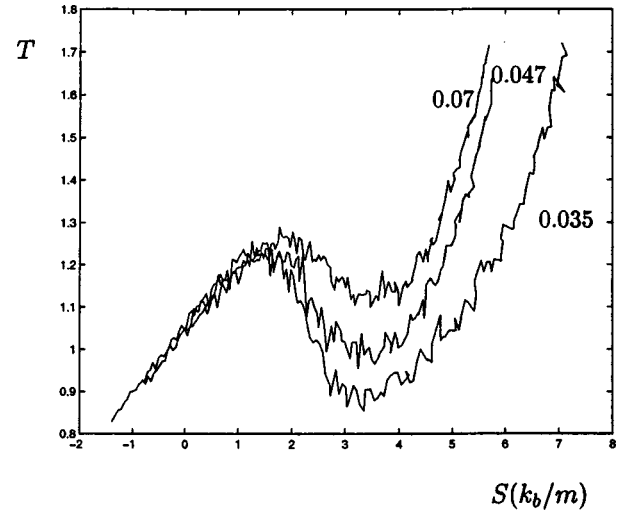


FIG. 4. Temperature as a function of entropy for the three different pressures indicated (in ϵ/σ^3).

$$S_Z = S_A + \int_A^Z \frac{dQ}{T} = S_A + \int_A^Z \frac{d(E + PV)}{T} \quad (13)$$

along the system path starting from A; here Z is any point on the system path. Since the integration does not need to be evaluated from both phases, the entropy and as a result the Gibbs free energy datum can be set arbitrarily. The entropy is set equal to zero at A (start of heating). The entropy of the fluid for simulations at a different pressure (introduced later) is determined consistently with the datum defined above, by using data from [9] to find the difference in entropy between the initial states of the two simulations.

The saturation temperature, T_{sat} , is defined by point O on the $G-T$ diagram of Fig. 3, or equivalently, by a ‘‘Maxwell construction’’ [10] on the $T-S$ diagram of the same figure. The value obtained ($T_{\text{sat}} = 1.18$) is close to the value cited in [11] (1.19) for MC simulations with a cut-off of 2.5σ , the full Lennard-Jones prediction (1.19) of Powles [11], and the (more accurate) MC predictions (1.18) of Lotfi, Vrabec, and Fischer [12]. The saturated liquid density ($0.59\sigma^{-3}$), and saturated gas density ($0.08\sigma^{-3}$) compare very well with the corresponding predictions of Powles [11], which are $0.59\sigma^{-3}$ and $0.12\sigma^{-3}$, respectively, and the predictions of Lotfi, Vrabec, and Fischer [12], which are $0.59\sigma^{-3}$ and $0.09\sigma^{-3}$, respectively.

Our results are also independent of the number of molecules in the system: the results for 960, 1920, and 3840 molecules are all indistinguishable from the results of Fig. 2 within the temperature uncertainty of our simulations

TABLE I. Vapor and liquid spinodals.

T	$\rho_{sp}(\sigma^{-3})$ (Simulation)	$\rho_{sp}(\sigma^{-3})$ (Theory)	Description
1.27	0.45	0.46	Liquid
1.14	0.14	0.15	Vapor
1.23	0.48	0.48	Liquid
0.99	0.12	0.12	Vapor
1.22	0.48	0.49	Liquid
0.89	0.08	0.10	Vapor

(± 0.03). Extensive series of simulations were performed to verify that all the results presented can be reproduced with the rescaling version of the heat addition equations [Eqs. (4) and (5)] both for constant volume and constant pressure. The reversibility of cooling simulations at constant pressure [$\dot{Q} = -3.125 \times 10^{-3} \varepsilon / (m\tau)$], for both the exact algorithm and its rescaling equivalent, has also been verified.

The above simulation was repeated at three different pressures (see Fig. 4). Table I shows the comparison between theoretical results [13] for the location of the liquid and vapor spinodal on a $T-\rho$ diagram and our simulation results. The second column gives the simulation result for the density as a function of the temperature, and the third column gives the results of [13] at the same temperature. The spinodal branch (vapor or liquid) is indicated in the fourth column. The agreement is very good indicating that we have recovered correctly the dynamics of the metastable system all the way to the spinodal.

In classical homogeneous nucleation theory the spinodal points are identified with the homogeneous nucleation limit [14]; before this limit is reached the system is in metastable states (segments BC and FH) in which a finite size disturbance in the form of a new-phase nucleus is required to initiate the phase transition. The states in the region CF are unstable; the fluid changes phase by spinodal decomposition in the presence of infinitesimal disturbances [14]. Spinodal decomposition has been observed in MD by Mruzik, Abraham, and Pound [15]. The disturbance wavelengths to which the fluid is unstable ($5-15\sigma$) are well within the reach of MD. One of the outstanding theoretical issues is the transition between homogeneous nucleation and spinodal decomposition.

The rate at which vapor nuclei are spontaneously produced in a liquid per unit time and per unit volume, $J(T, P)$, is given by the following relation [16]:

$$\log_{10} J(T, P) = a \{1 - e^{-(T-T_0)G/a}\}. \quad (14)$$

Note that this expression is an approximate curve fit to the various theories that predict nucleation rates, and that a and G are material constants that depend on the pressure; T_0 is the temperature for which

$$\log_{10} J(T_0, P) = 0. \quad (15)$$

(The condensation case is similar but somewhat less well characterized.) This nucleation rate rises steeply as the supersaturation ($T-T_0$) rises and it is easy to show that even for the high heating rates of our simulations the dominant contribution to the total number of formed nuclei will be from the highest temperature encountered. For argon, $J(T = T_C = 1.27, P = 0.07) \sim 1.2 \times 10^{-5} \sigma^{-3} \tau^{-1}$. One of the questions of interest to date is the success rate of these nuclei, or in other words, how many nuclei will have to be present before one successfully initiates the phase transition. If we assume that $O(10)$ nuclei are required, the heat addition timescale must be $\tau_T > 10\rho/[NJ(T_C, P = 0.07)] \sim 1000\tau$. In addition to that, the above [Eq. (14)] steady state relation is valid after a time of approximately $10^4\tau$ has passed in a given metastable state [16]. The current heat addition rates ($\tau_Q \sim 100\tau$), determined by our computer resources, cannot at this time allow the phase change by homogeneous nucleation.

We thus expect that because of the insufficient time spent at the homogeneous nucleation points, the fluid in our simulation changes phase by crossing into the unstable region where spinodal decomposition takes over. Further investigation of the dynamics of phase change, the clarification of various issues such as the existence of van der Waals type loops in the phase change history of fluids, as well as the extension of the theoretical framework to include constant pressure heat addition are the subjects of ongoing research.

This work was supported by DARPA and the ONR under Grant No. N00014-91-J-1889. The author thanks Professor William Hoover for helpful comments and suggestions.

-
- [1] W. G. Hoover, *Computational Statistical Mechanics* (Elsevier, Amsterdam, 1991).
- [2] D. J. Evans and G. P. Morriss, *Statistical Mechanics of Non-equilibrium Liquids* (Academic Press, New York, 1990).
- [3] H. J. Berendsen *et al.*, *J. Chem. Phys.* **81**, 3684 (1984).
- [4] W. G. Hoover, *J. Chem. Phys.* **109**, 4164 (1998).
- [5] M. P. Allen and D. J. Tildesley, *Computer Simulation of Liquids* (Oxford University Press, Oxford, 1987).
- [6] K. Refson, *Physica B* **131**, 256 (1985).
- [7] A. Tenenbaum, G. Ciccotti, and R. Gallico, *Phys. Rev. A* **25**, 2778 (1982).
- [8] M. Parinello and A. Rahman, *J. Appl. Phys.* **52**, 7182 (1981).
- [9] *Gas Encyclopaedia* (Elsevier, Amsterdam, 1976).
- [10] C. J. Adkins, *Equilibrium Thermodynamics* (McGraw-Hill, New York, 1968).
- [11] J. G. Powles, *Physica A* **126**, 289 (1984).
- [12] A. Lotfi, J. Vrabc, and J. Fischer, *Mol. Phys.* **76**, 1319 (1992).
- [13] W. E. Langlois and F. F. Abraham, *Chem. Phys. Lett.* **52**, 129 (1977).
- [14] V. P. Skripov, *Metastable Liquids* (Wiley, New York, 1974).
- [15] M. R. Mruzik, F. F. Abraham, and G. M. Pound, *J. Chem. Phys.* **69**, 3462 (1978).
- [16] V. P. Skripov *et al.*, *Thermophysical Properties of Liquids in the Metastable (Superheated) State* (Gordon and Breach, New York, 1988).